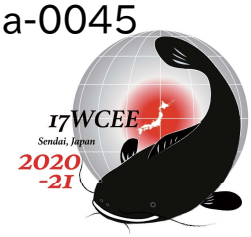

JOINT INVERSION OF SURFACE-WAVE PHASE AND GROUP VELOCITIES FOR EFFICIENT ESTIMATION OF DEEP S-WAVE VELOCITY STRUCTURES: KATHMANDU VALLEY, NEPAL

T. Hayashida[(1)], T. Yokoi[(2)], M. Bhattarai[(3)], and N. Maharjan[(4)]

[(1)] *Senior Research Scientist, IISEE, Building Research Institute, takumi-h@kenken.go.jp*
[(2)] *Senior Fellow, IISEE, Building Research Institute, Japan, tyokoi@kenken.go.jp*
[(3)] *Seismologist, DMG, Nepal, mb2058@yahoo.com*
[(4)] *Geologist, DMG, Nepal, nrshmhrjn72@gmail.com*

Abstract

The conventional microtremor array method focuses on deriving the dispersion characteristics of longer wavelength (2–10 times the array radius) Rayleigh-wave phase velocities to estimate subsurface S-wave velocity structure models. We demonstrated in a previous study that inter-sensor Green's functions can be extracted from a temporally deployed microtremor array in the Kathmandu Valley, Nepal, using the seismic interferometry technique and that shorter wavelength (1/10–1/2 times the inter-sensor distance) Rayleigh-wave group velocities can be stably estimated regardless of the azimuth angle. In this study, we apply our proposed method to other existing microtremor array data recorded in the Kathmandu Valley to investigate the possibility of a joint inversion of Rayleigh-wave phase and group velocities for efficient estimation of the S-wave velocity structure of deep sedimentary layers. The estimated S-wave velocity structure models from the joint inversion correspond well to those of existing results that were estimated using several different size arrays except one site where structural heterogeneity could exist. Our results indicate that our approach makes it possible to obtain surface-wave properties over a wide frequency range using limited microtremor data and can be a flexible tool to reduce the time and effort needed for actual surveys.

Keywords: Microtremor, Phase velocity, Group velocity, Seismic interferometry, Kathmandu Valley

1. Introduction

Microtremor (ambient noise/ambient vibration) survey methods have advantages in terms of cost and simplicity with respect to determinations of the subsurface S-wave velocity (Vs) structure. Surveys consist of various measurements (single points or circular, triangular, linear, L-shape, or irregular arrays) and analyses, including the horizontal-to-vertical (H/V) spectral ratio, spatial autocorrelation (SPAC), frequency–wavenumber, or centerless circular array (CCA) methods, such that survey plans need to be carefully designed considering the geological or geographical features of the target site and the performance of the equipment used in the survey. As for array exploration, conventional microtremor array data analyses aim to derive the dispersion curves of the surface-wave phase velocity and estimate an optimal seismic velocity structure model that accounts for the observed properties. The sizes of microtremor arrays range from several meters to several kilometers, depending on the target depths of interest. Several microtremor arrays with different sizes are needed when estimating the Vs structure from shallow to deep sediments, requiring large amounts of time or large numbers of sensors.

In the field of seismology, seismic interferometry has been widely used over the last decade as a tool to estimate seismic velocity structures [1, 2]. This methodology is usually based on a cross-correlation analysis of the ambient seismic noise (i.e., long-period microtremors generated mainy by ocean waves) recorded at two different broadband seismic stations and the extraction of surface-wave Green's functions along the interstation paths. This approach primarily focuses on the retrieval of shorter wavelength (one-third of the interstation

distance or less [3]) surface waves, while microtremor array surveys extract longer wavelength surface waves compared to the inter-sensor spacings (e.g., 2–10 times the inter-sensor distances for the SPAC method [4]). The first step of both the SPAC and seismic interferometry methods is to derive the cross-spectrum of the seismic noise recorded at two different points; however, their target wavelengths, inter-sensor distances, and the resultant frequency ranges are entirely different.

In theory, under the condition that the sources of the ambient seismic noises generating both short- and long-period surface waves are uniformly distributed outside of the array, both the SPAC and seismic interferometry methods can be applied to the same dataset to obtain the surface-wave properties over a broader range of wavelengths. Recent studies have tried to incorporate both methods [5–9]; however, the number of relevant examples is limited because there is no clear indicator of a reasonable measurement time and frequency range; in addition, there are difficulties in the treatment of nonuniform noise sources and the interpretation of the derived Green's functions. In a previous study in the Kathmandu Valley, Nepal, at site SDB (Fig. 1), we demonstrated that (1) the interstation Green's functions can be successfully extracted from microtremor arrays (sensor-to-sensor distances = 241–801 m), (2) the dispersive characteristics of the Rayleigh-wave group velocity can be derived in the higher frequency range, and (3) the required measurement time for seismic interferometry is at least several hours [10]. These findings indicate that both the surface-wave phase and group velocities can be extracted from the same dataset, making it possible to conduct a joint inversion to estimate the subsurface velocity structure from shallower to deeper depths. In this paper, we further apply the joint inversion using microtremor data recorded at five sites in the Kathmandu Valley and discuss technical issues in actual applications.

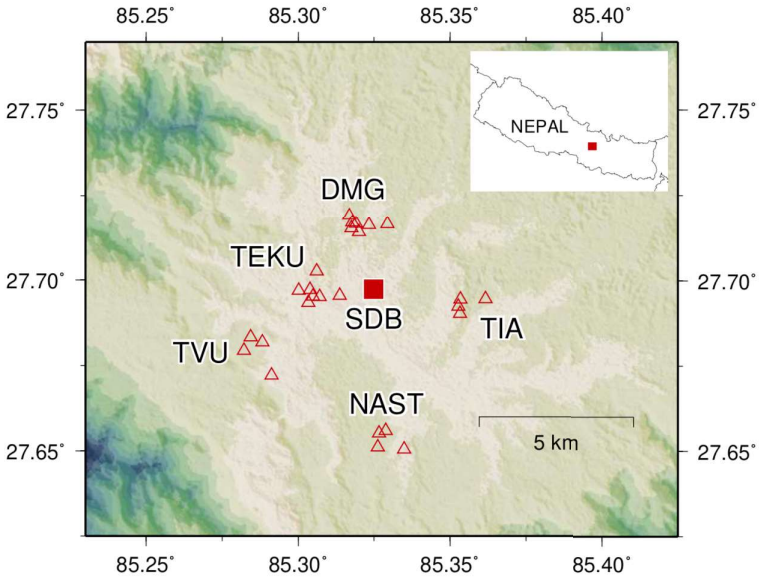

Fig. 1 – Locations of microtremor arrays in the Kathmandu Valley

2. Kathmandu Valley

The Kathmandu Valley, located in central Nepal, is a major tectonic basin in the Himalayas. The 660-km^2 basin, measuring approximately 20 km from east to west and 35 km from north to south, is the most populated area in Nepal and includes major cities such as Kathmandu, Bhaktapur, and Latipur. This basin contained a large lake from the late Pliocene to the Quaternary periods, and the current topography was formed during the Himalayan orogeny (20–2 Ma) [11,12]. A former gravity survey showed the existence of a thick (~650 m) sedimentary layer consisting of ancient lake sediments [13]. During the 2015 Gorkha earthquake (Mw 7.8), relatively long-period (3–5 s) ground motions were observed in the horizontal components inside the basin [14–16], implying ground-motion amplification due to the sediments. Aftershock recordings in the basin indicated the existence of thick (> 300 m), low-velocity (Vs < 1,000 m/s) sediments and a significant velocity contrast between the sediments and the bedrock layers [17]. Our microtremor survey results also indicate the existence of thick sedimentary layers in the central part of the basin [18–20].

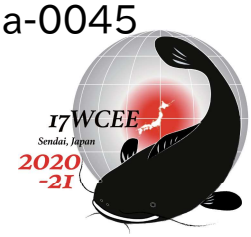

3. Data

We investigated the possibility of a surface-wave group velocity estimation using the existing microtremor data recorded in the Kathmandu Valley. We deployed irregular-shaped arrays at five sites: DMG, NAST, TEKU, TIA, and TVU (see locations in Fig. 1). At each site, microtremor measurements were conducted using several different size arrays [19]. Here we only used data for which the inter-sensor distances were larger than 100 m. We used four sets of portable broadband seismometers (CMG-40T, 800 V/m/s sensitivity; Gularp Inc.) and data loggers with a 24-bit A/D converter (DATAMARK LS-8800; Hakusan Corp.) for each measurement. The sampling frequency was set to 100 Hz. Each measurement lasted for more than 10 h (Table 1). The minimum and maximum sensor-to-sensor distances were 126 m and 1,400 m, respectively (see Table 1). The Vs structures of the deep sedimentary layers at each site were already estimated using the CCA method in the previous study [19].

Table 1 – Measurement time and array size

Array	Time		r_{min}	r_{max}
	Start	End		
DMG-1	2016/12/12 22:00	2016/12/13 09:00	126	1274
DMG-2	2016/12/13 15:00	2016/12/14 10:00	183	713
DMG-3	2016/12/14 15:00	2016/12/15 11:00	206	637
TEKU-1	2017/02/16 20:00	2017/02/17 08:00	826	1333
TEKU-2	2017/02/17 20:00	2017/02/18 09:00	209	425
TVU	2017/12/10 17:00	2017/02/11 09:00	423	1400
TIA	2018/12/09 20:00	2018/12/10 08:00	233	949
NAST	2018/12/10 17:00	2018/12/11 08:00	235	968

4. Application of Seismic Interferometry to Microtremor Recordings

First, we derived the inter-sensor Green's functions at the five sites using the seismic interferometry technique. The vertical components of the recorded microtremor data were used to derive the Green's functions. The time window used for the cross-correlation analysis was 81.92 s, with 50% overlapping. The recorded microtremor data were one-bit normalized after the removal of the offset and linear trend for each segment. The normalized waveforms were converted to frequency domain data using the fast Fourier transform, and the spectral amplitudes were whitened [21] using the absolute value of the complex spectra after smoothing with a 0.1-Hz Parzen window. The cross-correlation functions (CCFs) between two sensors were computed from the cross-spectra. Here, we regard the stacked CCFs as the Green's functions between the sensors and use the averaged waveforms for the negative and positive parts of the CCFs in the following analyses (see an example in Fig. 2). Distinct phases are clearly seen in the CCFs, indicating the possibility of seismic interferometry applications to microtremor data.

We next estimated the group velocities of the Rayleigh waves at the five sites, assuming that the surface-wave was dominant in the distinct wave trains. The group velocities obtained using a multiple filter analysis [22] indicated significant scattering both in the lower (< 0.5 Hz) and higher (> 5 Hz) frequency ranges, likely resulting from too-short or too-long wavelengths for the various array sizes; however, the values were stable within a certain frequency range. For example, for array TIA (Fig.2), the CCFs provide similar group velocities regardless of the azimuth angle in the frequency range between 2 and 5 Hz, while the estimated group velocities from shorter distance (< 300 m) CCFs were substantially smaller below 4 Hz and CCFs with the longest distance (949 m) could not show reasonable group velocities above 3 Hz. When we limit the available range

of frequencies such that the wavelengths are between 1/2 and 1/10 of the inter-sensor distances, assuming that the phase velocity is approximately 1.4 times the estimated group velocity, the estimated group velocities show dispersive characteristics. The estimated group velocities sometimes show large variations for different sensor pairs, possibly indicating the effect of a three-dimensional velocity structure or a nonuniform distribution of the ambient noise sources. Here, we incorporated the estimated group velocities for all pairs to obtain a dispersion curve at each site.

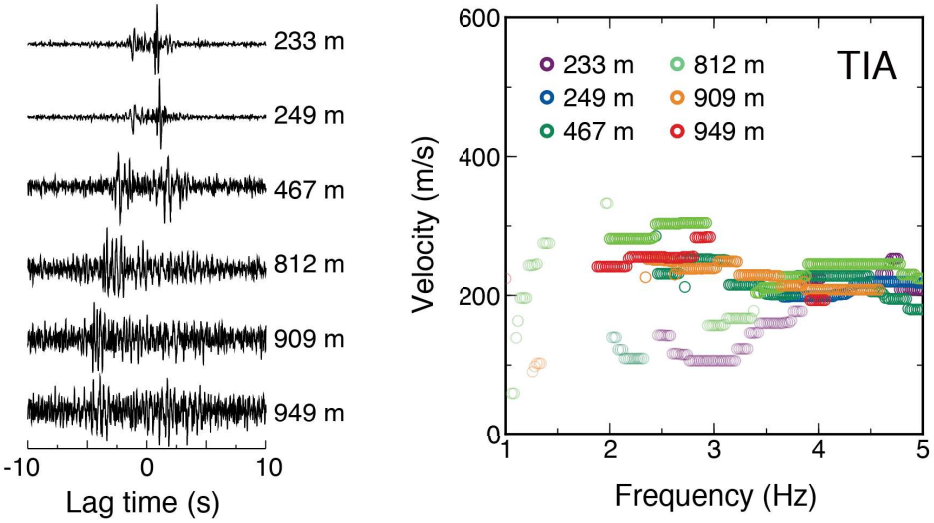

Fig. 2 – Examples of stacked cross-correlation functions (left) and estimated group velocities (right).

5. Joint Inversion of Rayleigh-wave Phase and Group Velocities

We estimated the Vs structures at the five sites using the derived Rayleigh-wave group velocities, as well as the phase velocities. The initial velocity structure consisted of six layers, and the range of the layer thickness and Vs values were the same as those in the previous study (Table 2). The P-wave velocities and densities of each layer were assigned using the conventional relationships [23,24]. We used a hybrid method combining the downhill simplex method [25] and the simulated annealing (SA) algorithm [26] to find an optimal model that minimizes the observed and theoretical phase and group velocities [27]. In the SA inversion, the cooling schedule is defined as

$$T = T_0 \exp\left(-ck^a\right) \tag{1}$$

where T is the temperature and T_0 is the initial temperature in Kelvin, k is the number of iterations at each temperature step, and a and c are constant coefficients. Here, we assigned $T_0 = 1.0$, $k = 5$, $a = 0.6$, and $c = 1.3$, respectively. The heuristic method finds the optimum values for 5,000 temperature changes. The misfit values were evaluated as follows:

$$\phi_C = \frac{1}{N_C}\sum_{n=1}^{N_C}\left(\frac{C_n^{obs} - C_n^{syn}}{\sigma_n^C}\right)^2 \tag{2}$$

$$\phi_U = \frac{1}{N_U}\sum_{n=1}^{N_U}\left(\frac{U_n^{obs} - U_n^{syn}}{\sigma_n^U}\right)^2 \tag{3}$$

$$\phi = p\phi_C + (1-p)\phi_U \tag{4}$$

where C^{obs} and C^{syn} are the observed and theoretical phase velocities; U^{obs} and U^{syn} are the observed and theoretical group velocities; φ_C and φ_U are the differences between the observed and theoretical phase and group velocities; and σ^C and σ^U are the standard deviations of the observed phase and group velocities, respectively. The weight coefficient p is defined as

$$p = \frac{N_C}{N_C + N_U} \tag{5}$$

where N_C and N_U are the numbers of data points for the observed phase and group velocities, respectively.

The estimated velocity structures and the comparisons between the derived and theoretical group and phase velocities for the final models are shown in Figures 3 and 4, respectively. The estimated structure models correspond well with those of previous studies that included results from smaller arrays to constrain the phase velocities in the higher frequency range, indicating that the joint inversion provides reasonable estimations of the subsurface Vs structure without deploying smaller arrays (with radii of less than 100 m) for estimating Vs in the shallower part. In addition, the agreements between the observed and theoretical phase and group velocities were found to be satisfactory, showing the suitability of using group velocities from the same microtremor arrays and the effectiveness of the joint inversion. Conversely, the estimated depths of the bedrock layer (Vs > 1,000 m/s) in this study differ slightly from those of previous models. This is because the determined phase velocities possibly have a low resolution at the bedrock depth. Structure model estimations using phase velocities over a much lower frequency range (0.01–0.2 Hz), which are derived from teleseismic signals [28], may yield a better resolution for deeper structures [19].

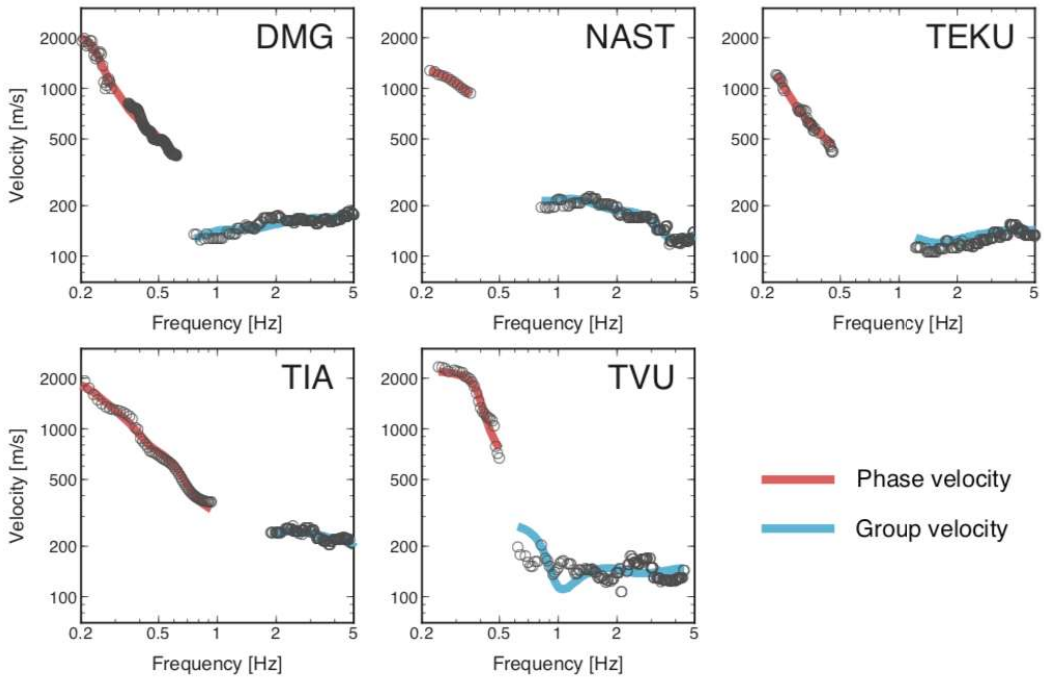

Fig. 3 – Observed phase and group velocities (circles) and the theoretical values from the final models (Phase velocity: red lines, Group velocity: blue lines).

Table 2 – Search range used for the model inversion

Layer	Vs (m/s)	Thickness (m)
1	150 – 250	10 – 300
2	200 – 300	50 – 300
3	350 – 500	50 – 300
4	400 – 800	50 – 400
5	700 – 1000	50 – 600
6	1000 – 3200	–

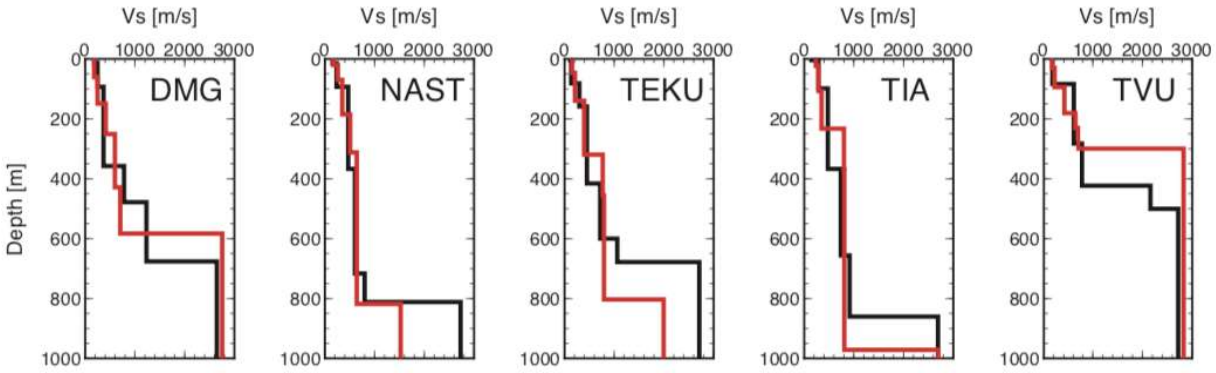

Fig. 4 – Estimated S-wave velocity structure models (black: only phase velocities with small–large size arrays, red: joint inversion with only larger arrays).

6. Theoretical H/V Spectral Ratios

We demonstrated that the application of seismic interferometry using microtremor array data can provide useful information to constrain the shallow subsurface structure and reduce the effort involved in a survey. On the other hand, the estimated bedrock depths in our study are different from previous results (Fig. 4), indicating uncertainty in the deeper structures. In general, deep sedimentary layers control the site response characteristics in the lower frequency range, and the effects are seen as spectral peaks in the microtremor horizontal-to-vertical spectral ratios (MHVRs). In the Kathmandu Valley, we found that observed MHVRs show predominant peak at frequencies lower than 1 Hz, reflecting the clear seismic velocity contrast between the bedrock and the sediments [20]. To investigate the reliability of the deep sedimentary velocity structure, we computed MHVRs for each site and compared them with the theoretical ones (Fig. 5). The time windows used in the MHVR calculations were 81.92-s long, with 50% overlapping. The black traces in Figure 5 show the MHVRs for each observation point. Except for site TVU where the observed MHVRs showed different peaks at each observation point, the observed MHVRs showed similar tendencies, implying small structural variations inside the arrays.

Next, we computed theoretical spectral ratios with the estimated Vs structure models using the ellipticity of Rayleigh waves, assuming that fundamental-mode surface waves dominate the microtremor data [29]. All the theoretical spectral ratios have dominant frequencies in the lower frequency ranges; however, the estimated dominant frequencies are slightly lower than the observed dominant frequencies. The theoretical spectral ratios from the previously estimated models also indicated similar discrepancies regardless of the bedrock depth differences between the models, implying shallower bedrock depths or insufficient physical parameters of subsurface layers (Vp or density). These comparisons may also indicate that the contributions of deeper structural differences might not be significant for our joint inversion results and that further approaches (e.g.,

the use of phase velocities at much lower frequencies or joint inversions of surface-wave dispersions and H/V properties) are required to constrain the bedrock depth over the entire survey area.

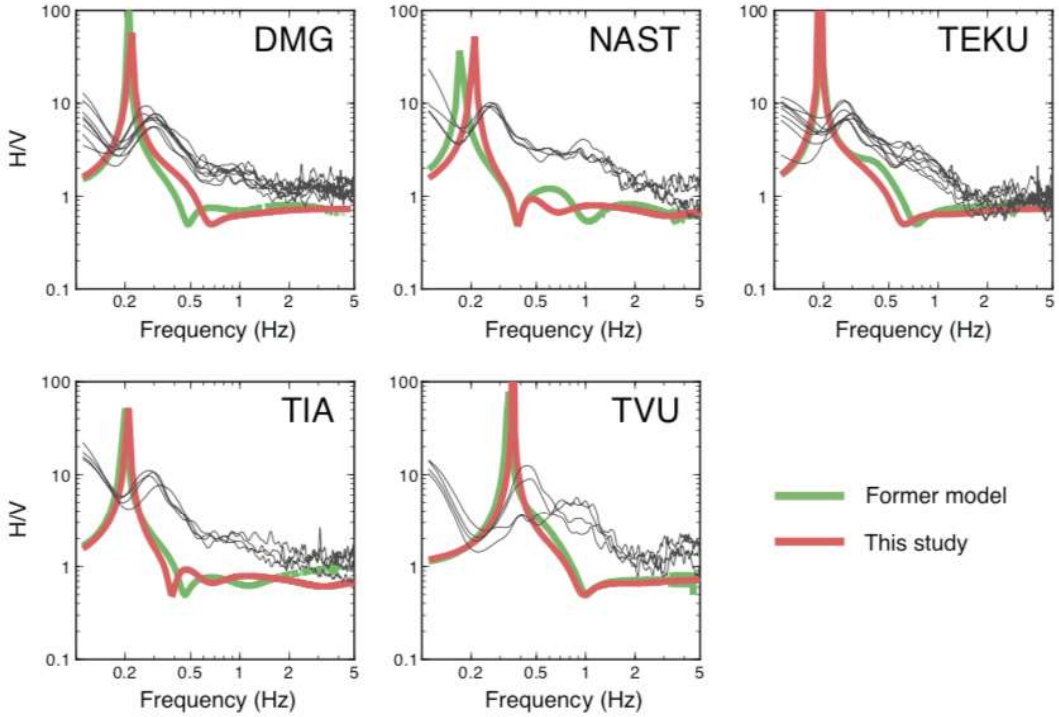

Fig. 5 – Observed microtremor horizontal-to-vertical (H/V) ratios (black traces) and synthetic H/V ratios of surface waves using different structure models (green: previous study, red: this study).

7. Conclusions

We applied seismic interferometry to microtremor array data recorded at five sites in the Kathmandu Valley, Nepal. The results indicate that (1) inter-sensor Green's functions can be extracted from noise CCFs, (2) the group velocities of the Rayleigh-wave can be determined from the derived Green's functions, and (3) the joint inversion of the Rayleigh-wave phase and group velocities provides a good estimation of the subsurface Vs structure without using smaller array ($r < 100$ m) data. Our proposed approach would reduce survey time and effort and could be a useful tool for actual surveys.

8. Acknowledgements

This study was supported by Japan Science and Technology Agency and Japan International Cooperation Agency under the "Science and Technology Research Partnership for Sustainable Development (SATREPS): Integrated Research on Great Earthquakes and Disaster Mitigation in Nepal Himalaya (FY2016-2020)." Microtremor surveys were performed with help from DMG experts.

9. References

[1] Shapiro NM, Campillo M (2004): Emergence of broadband Rayleigh waves from correlations of the ambient seismic noise. Geophysical Research Letters, 31, L07614.

[2] Sabra KG, Gerstoft P, Roux P, Kuperman WA (2005): Extracting time-domain Green's function estimates from ambient seismic noise. Geophysical Research Letters, 32, L03310.

[3] Lin FC, Moschetti MP, Ritzwoller MH (2008): Surface wave tomography of the western United States from ambient seismic noise: Rayleigh and Love wave phase velocity maps, Geophysical Journal International, 173, 281-298.

[4] Cornou C, Ohrnberger M, Boore DM, Kudo K, Bard PY (2006): Derivation of structural models from ambient vibration array recordings: result from an interpretational blind test, Proceedings of the 3rd International Symposium on the Effects of Surface Geology on Seismic Motion, Grenoble, France.

[5] Yokoi T (2010): New formulas derived from seismic interferometry to simulate phase velocity estimates from correlation methods using microtremor, Geophysics, 75 (4), SA71-SA83.

[6] Chávez-García, FJ, Yokoi T (2015): High lateral resolution exploration using surface waves from noise records, Exploration Geophysics, 47 (2), 123-132.

[7] Chimoto K, Yamanaka H (2013): Applicability of estimation of Rayleigh-wave group velocities by using seismic interferometry in the short-period range, BUTSURI-TANSA, 66 (3), 179-188 (in Japanese with English abstract).

[8] Hayashida T, Yoshimi M (2014): Validation of S-wave velocity structure by application of seismic interferometry and SPAC method to long-term microtremor array data, Proceedings of the 15th Japan Earthquake Engineering Symposium, Chiba, Japan (in Japanese with English abstract).

[9] Tsuno S, Iwata N, Miyakoshi H, Yamamoto S, Chimoto K (2015): An application case of seismic interferometry to exploration of subsurface layer, using short-period microtremor, Journal of Japan Association for Earthquake Engineering, 15 (7), 7_454-7_462 (in Japanese with English abstract).

[10] Hayashida T, Yokoi T, Bhattarai M (2019): Estimation of shallow-to-deep shear wave velocity structure from joint inversion of surface-wave phase and group velocities, Journal of Japan Association for Earthquake Engineering, 19 (5), 111-124 (in Japanese with English abstract).

[11] Sakai H, Fujii R, Kuwahara Y, Noi H (2000): Climatic changes and tectonic events recorded in the Paleo-Kathmandu Lake sediments, Journal of Geography, 109 (5), 759-769 (in Japanese with English abstract).

[12] Sakai T, Gajurel AP, Tabata H (2016) Seismites in the Pleistocene succession and recurrence period of large earthquakes in the Kathmandu Valley, Nepal, Geoenvironmental Disasters, 2, Paper no.25.

[13] Moribayashi S, Maruo Y (1980): Basement topography of the Kathmandu Valley, Nepal, Journal of the Japan Society of Engineering Geology, 21 (2), 80-87.

[14] Dixit AM, Ringler AT, Sumy DF, Cochran ES, Hough SE, Martin SS, Gibbons S, Luetgert JM, Galetzka J, Shrestha SN, Rajaure S, McNamara DE (2015): Strong-motion observations of the M7.8 Gorkha, Nepal, earthquake sequence and development of the N-SHAKE strong-motion network, Seismological Research Letters, 86 (6), 1533-1539.

[15] Bhattarai M., Adhikari, L.B., Gautam, U.P., Laurendeau, A., Labonne, C., Hoste-Colomer R., Se7\be O. and Hernandez B (2015): Overview of the large 25 April 2015 Gorkha, Nepal, earthquake from accelerometric perspectives. Seismological Research Letters, 86 (6), 1540-1548.

[16] Takai N, Shigefuji M, Rajaure S, Bijukchhen S, Ichiyanagi M, Dhital MR, Sasatani T (2015): Strong ground motion in the Kathmandu Valley during the 2015 Gorkha, Nepal, earthquake, Earth, Planets and Space, 68, Paper no. 10.

[17] Bijukchhen SM, Takai N, Shigefuji M, Ichiyanagi M, Sasatani T, Sugimura Y (2017): Estimation of 1-D velocity models beneath strong-motion observation sites in the Kathmandu Valley using strong-motion records from moderate-sized earthquakes, Earth, Planets and Space, 69, Paper no. 97.

[18] Bhattarai M, Nepali D, Dhakal S, Shrestha S, Yokoi T, Hayashida T (2017): Microtremor array exploration for deep sedimentary layers in the central part of the Kathmandu Valley, Nepal, JAEE Annual Meeting, Tokyo, Japan.

[19] Yokoi T, Hayashida T, Bhattarai M, Pokharel T, Dhakal S, Shrestha S, Timsina C, Bhattarai S, Sharma R, Nepali D (2020): Broadband microtremor array exploration in Kathmandu Valley, Nepal, 17WCEE, Sendai, Japan.

[20] Maharjan N (2018): Investigation of Site Response in Kathmandu Valley Using Aftershock Data of the 2015 Gorkha Earthquake, Nepal, Master Thesis, National Graduate Institute for Policy Studies, Tokyo, Japan.

[21] Bensen GD, Ritzwoller MH, Barmin MP, Levshin AL, Lin F, Moschetti MP, Shapiro NM, Yang Y (2007): Processing seismic ambient noise data to obtain reliable broadband surface wave dispersion measurements, Geophysical Journal International, 169 (3), 1239-1260.

[22] Dziewonski A, Bloch S, Landisman M (1969): A technique for the analysis of transient seismic signals, Bulltein of the Seismological Society of America, 59 (1), 427-444.

[23] Kitsunezaki C, Goto N, Kobayashi Y, Ikawa T, Horike M, Saito T, Kurota T, Yamane K, Okuzumi K (1990): Estimation of P- and S- wave velocities in deep soil deposits for evaluating ground vibrations in earthquake, Journal of Japan Society for Natural Disaster Science, 9 (3), 1-17 (in Japanese with English abstract).

[24] Ludwig WJ, Nafe JE, Drake CL (1970): Seismic refraction, The Sea, 4, Wiley Interscience, 53-84.

[25] Nelder JA, Mead R (1965): A simplex method for function minimization, The Computer Journal, 7 (4), 308-313.

[26] Ingber L (1989): Very fast simulated re-annealing, Mathematical and Computer Modelling, 12 (8), 967-973.

[27] Yokoi T (2005): Combination of downhill simplex algorithm with very fast simulated annealing method -An effective cooling schedule for inversion of surface wave's dispersion curve-, Seismological Society of Japan 2005 Fall Meeting, Sapporo, Japan (in Japanese).

[28] Hayashida T, Yokoi T, Bhattarai M, Dhakal S, Shrestha S, Pokharel T, Maharjan N, Timsina C (2019): Estimation of bedrock depth in the Kathmandu Valley, Nepal, using ambient noise and teleseismic Data, Seismological Society of Ametica Annual Meeting, Seattle, WA, USA.

[29] Arai H, Tokimatsu K (2005): S-wave velocity profiling by joint inversion of microtremor dispersion curve and horizontal-to-vertical (H/V) spectrum, Bulltein of the Seismological Society of America, 95 (5), 1766-1778.

